Journal of New Technology and Materials (JNTM)
J. New Technol. Mater.
Vol. 09, N°02 (2019)28-34

OEB Univ. Publish. Co.

Influence of cold deformation on the aging behavior of the Al-Mg-Si alloy

Y. Aouabdia[a,*], L. Amiour[b] and A. Boubertakh[b]

[a]*Ecole Normale Supérieure de Constantine, Assia Djabar, Ali Mendjeli, Constantine 25000, Algeria*
[b]*Physics department, Faculty of Exact Sciences, University of Mentouri Constantine 1, Ain El bey Road, Constantine 25000, Algeria*

* Corresponding author, email: youcefaouabdia@yahoo.fr

Received date: June 26, 2019 ; revised date: Sep. 29, 2019 ; accepted date: Oct. 27, 2019

Abstract

The aim of the present work is to study the effect of the cold deformation followed by heat treatment on the microstructure and the mechanical properties of an Al-Mg-Si alloy. Differential scanning calorimetry indicates that precipitation of the metastable β" phase occurs in the temperature range (220-260 °C) for the solution treated and then quenched alloy to room temperature. The exploitation of the DSC curves by the Kissinger method has shown that the activation energy value of the precipitation reaction is about 83.1 k J / mol. The amount of 30% cold deformation before aging indicates that the first dissolution reaction at about 50°C and the precipitation temperature is around 240 °C. Microstructural studies, of the aged cold-deformed sample, revealed the presence of fine precipitates embedded in the α–aluminium matrix. At as quenched state of the alloy reveals an aging response. The increase of the microhardness with the decrease of the elongation is mainly due to the severe strengthening by deformation, and not to the effect of precipitation hardening.

Keywords: Cold deformation, Al-Mg-Si Alloys, β' phase, activation energy, precipitation, hardening;

1. Introduction

Aluminum alloys are selected as structural application materials because of their lightweight, high strength and stiffness, corrosion resistance and for their ability to undergo an aging hardening [1-4].

The latter alloys are mainly used in the automotive and low-temperature aeronautical industries because they lose their strength at high temperature [3]. Elements such as copper, manganese, magnesium, zinc, nickel and silicon are the major additive for aluminum to satisfy the different requirements of use. These elements improve the properties of aluminum when added with suitable percentages [4-6]. For example, silicon addition in the range 0.53-1.80 wt.% makes the aluminum alloy Al 6083 more sensitive to artificial aging [6]. In the above alloy, hardening is realized through the precipitation process and often characterized by the qualitative knowledge of the precipitation sequence and its influence on the mechanical properties [7-10]. Precipitation hardening is an important key mechanism that enables Al-Mg-Si alloys to provide better properties [11-12].

The precipitation sequence of Al-Mg-Si alloys during aging can be generally expressed as:

Solid Supersaturated Solution (SSS) → GP (Guinier-Preston) zones →β″→β' →β(Mg_2Si) [8, 9,13,14].

Recent needs in automotive and aeronautic industries require a reduction in weight and cost with an improvement in micro-tension, tensile strength and yield strength for the commercial aluminum alloys. The performance of the alloys depends heavily on the design of the thermo-mechanical processing route. Cold deformation before aging is the most efficient method in industry.

Many authors have reported that differential scanning calorimetry (DSC) allowed them to follow phase transformations of the precipitation sequence in these alloys [10-12]. Among the analogical methods, the Kissinger one is the most practical for determining some kinetic parameters, such as the activation energy, on the basis of the different heating rates that correspond to the peaks observed in the DSC curves [15, 16].

Aging treatments intend to change the nature and distribution of the constituents of materials. Depending on the field of application of the material, the heat treatments can improve or deteriorate the mechanical properties. The present work aims to reveal the effect of cold deformation on microstructural evolution and mechanical properties of an Al-Mg-Si alloy during natural and artificial aging. The Kissinger method is also used to estimate the activation energy of the precipitation processus in this alloy using the DSC technique.

2. Experimental procedure

The chemical composition of the studied aluminum alloy is shown at Table 1. The cast aluminum alloy, of ~29.5 mm thickness, was homogenized at 550 °C for 1h. After water quenching, a series of samples were

immediately cold rolled to 20 and 30% of reduction rates.

Table 1: Chemical composition of the alloy under study

Element	Mg	Si	Cu	Fe	Mn	Al
Wt.(%)	1.08	0.54	0.31	0.11	0.05	bal

Cold-deformed samples as well as those produced were subjected to DSC to study the precipitation using different heating rates ranging from 5 to 20 °C/min from ambient to 500 °C, and cooling to room temperature with the same speed as the heating rate. Samples have a cylindrical shape of the hollow form and a mass of around 15 mg that is approximately the same of the reference sample. The differential calorimetric analyzes were carried out by METTLER 4000-TC 11 instrument. Samples prepared for metallographic microscopy were mechanically polished and then chemically etched by the universal standard electrolytic reagent. In our work, the optical microscope used is of type Zeiss Axiovert 40 Mat and the scanning electron microscopy is a JEOL, JSM-5510, it is equipped with an energy-dispersive x-ray (EDS) system to determine the chemical composition of precipitates. For microhardness measurements, a Brinell Cum Vickers hardeness tester (model: BV-250 (SPL)) was used. Some selected samples have been submitted to tensile strength tests using an Instron 4204 (Zwik/Roell) machine under un elongation speed of $6{,}66.10^{-5}$ s^{-1}. Samples have been prepared according to the standard norm ASTM (ASTM: Vol.03.01: E8M-96).

3. Results and discussions

3.1 DSC study

Figure 1 shows DSC thermograms obtained using heating rates ranging from 5 to 20 °C/min, homogenized samples were then water quenched. For the heating rate of 5 °C/min, one can observe the appearance of a large peak at ~245 °C, even at 254, 258 and 266 °C for the other heating rates 10, 15 and 20 °C/min, respectively. It is clear that the DSC peak shifts to higher temperatures as the heating rate increases. It is important to mention here that the curve corresponding to the heating rate 5 °C/min, shows the first exothermic peak at around 56 °C followed by two exothermic peaks at 243 °C and 292 °C. It can be assumed that the first peak is attributed to the formation of GP zones [17, 18]. This peak is immediately followed by an endothermic peak indicating the dissolution of the GP zones.

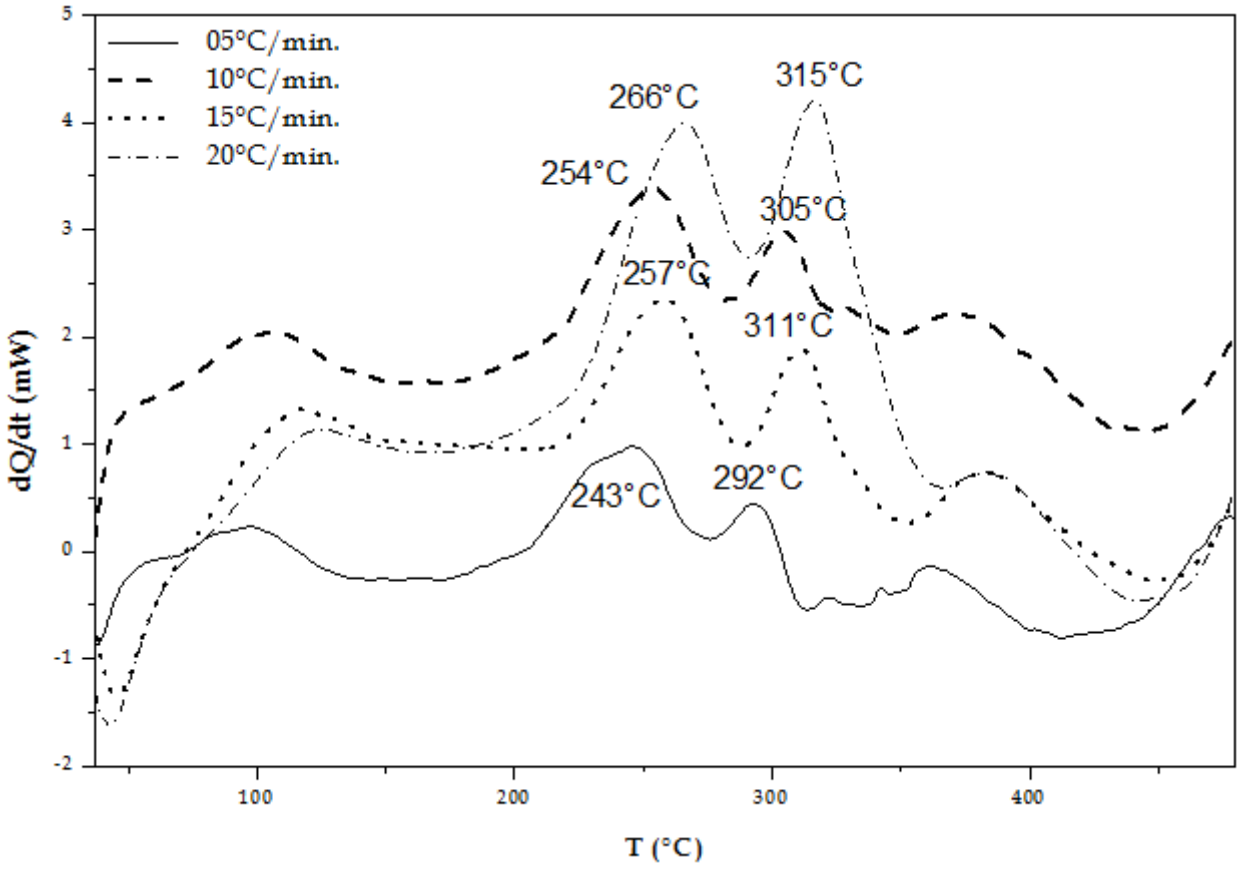

Figure 1. DSC Curves obtained with different heating rates of the homogenized and quenched samples.

The second exothermic peak (~243 °C) corresponds to the precipitation of the β" phase, and the third peak at 292 °C is attributed to the formation of the β' phase, which is in agreement with many papers [19, 20]. However, the thermograms of figure 1 don't show the first exothermic peak in the case of higher heating rates (> 15 °C/min) due to the gradual dissolution of GP zones which disappear completely at 71 °C [20].

The variation of the maximum peak temperatures (T_{max}) as a function of the heating rate (ϕ) determines directly

the activation energy of the reaction. We have used the Kissinger method [15-16], for determining the activation energy :

$$\ln\frac{\phi}{T_{max}^2} = -\frac{E_{act}}{RT_{max}} + C$$

Where R (8.314 J/mol) is the gas constant. The activation energy determined is fed into the fitting procedure and ultimately a set of parameters characteristic of the reaction are obtained.

Table 2 summarizes all the parametric values of β" phase precipitation, of the homogenized and quenched alloys. Figure 2 shows the curve that determines the activation energy by the Kissinger method and using the data summarized in Table 2. From Figure 2, the slope ($-E_{act}/R$) is about (-9951.8), so the activation energy is found: E_{act} = 8.314 x 9951.8 = 83.1 kJ/mol. The activation energy calculated in the present work is in good agreement with the value reported for an air-cooled aluminum alloy Al 6083, using the Kissinger method.

Figure 3 shows the DSC curve obtained with a heating rate of 10 °C/min for the alloy subjected to a cold deformation of 30%. The comparison with the undeformed alloy, i.e. homogenized and quenched alloy, with the same heating rate (10°C / min) of figure 1, clearly identifies that no acute peak of DSC was obtained for the cold-deformed specimen, except one at 240°C which may be linked to the formation of β" and/or β' as reported in literature [21, 22].

Table 2: Linked parameters for each peak of the homogenized and then quenched alloy using Kissinger method.

Heating rate (°C/min)	Peak(°C)	T(K)	$Ln(\phi/T^2_{max})$	$(1/T_{max})$
5	243	516	-14.1	0.00175
10	254	527	-14.4	0.00173
15	257	530	-13.5	0.00171
20	266	539	-13.4	0.00169

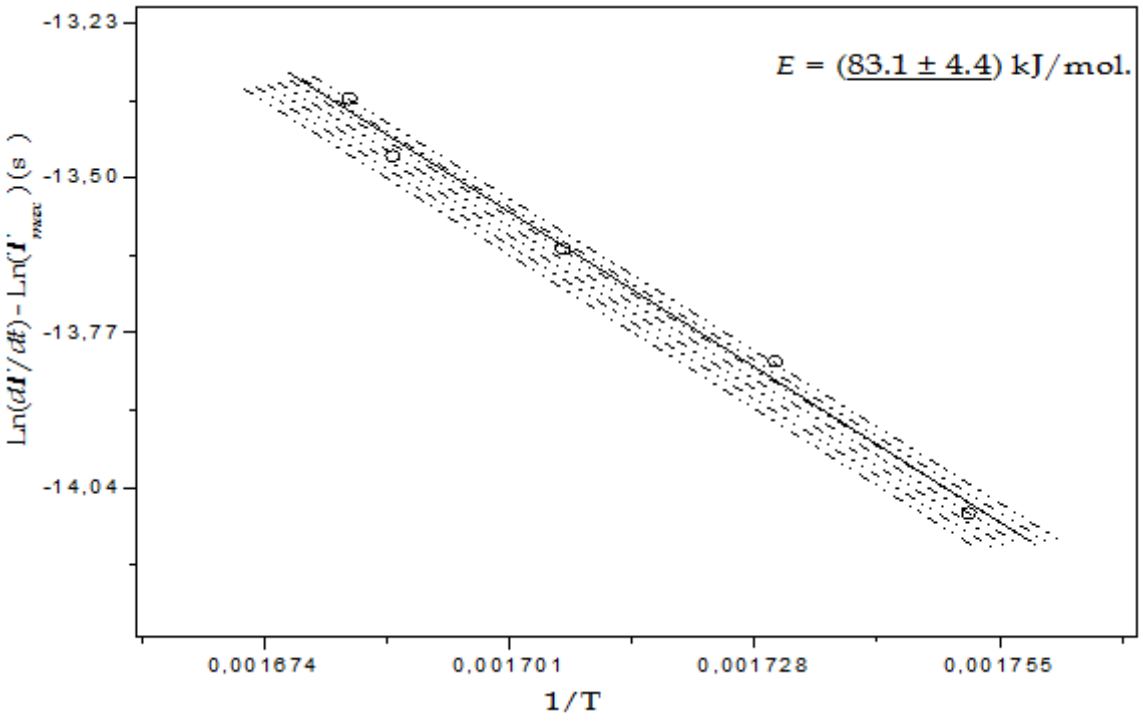

Figure 2. Kissinger diagram for determining the activation energy obtained of the homogenized alloy.

The absence of the first peak, which is linked to the formation of GP zones, is attributed to the dissolution of fine or possible clusters at certain PG areas formed at ambient temperature. It is assumed that the time lag between quenching and DSC measurements causes natural aging and leads to the dissolution reaction at about 55 °C [23, 24].

The precipitation reaction (at ~240 °C) may be also attributed to either phase (β") and/or (β'). The peak (at ~420 °C) is most likely attributed to the formation of β phase (Mg_2Si) [25, 26]. Subsequently, the slope of the curve is upward until it is balanced. Effectively, cold deformation can be considered to cancel out of the gap sites, while introducing heterogeneous nucleation sites, i.e. dislocations for precipitation. Therefore, the presence of an important density of dislocations generated by cold deformation reduces the activation energy that can lead to the beginning of β "or β ' phase formation at lower temperature (~ 240 ° C).

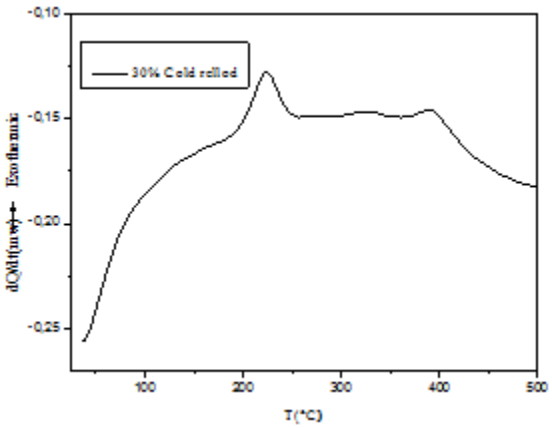

Figure 3. DSC thermogram obtained with a heating rate of 10°C/min for the 30% cold rolled alloy.

3.2 Microstructures

The optical micrograph of the artificially aged aluminum alloy is shown in Figure 4. It shows fine spots of different sizes, which uniformly distributed in the matrix. It is a mixture of the matrix α and very probably the precipitates Mg_2Si phase [19].

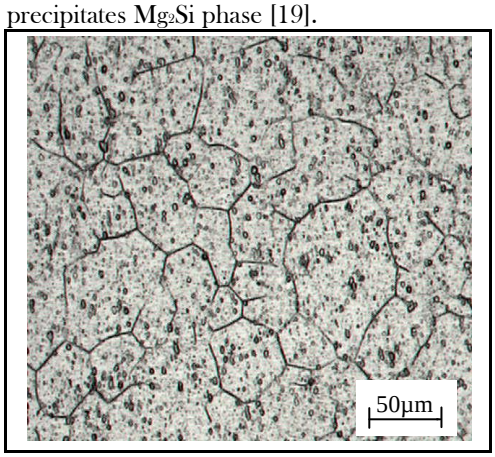

Figure4. Optical micrograph of the artificially aged alloy at 175°C for 12 hours.

Figure 5a presents the SEM image of the 30% cold rolled alloy. It shows also the presence of fine precipitates (black spots) within the α-aluminum matrix grains.

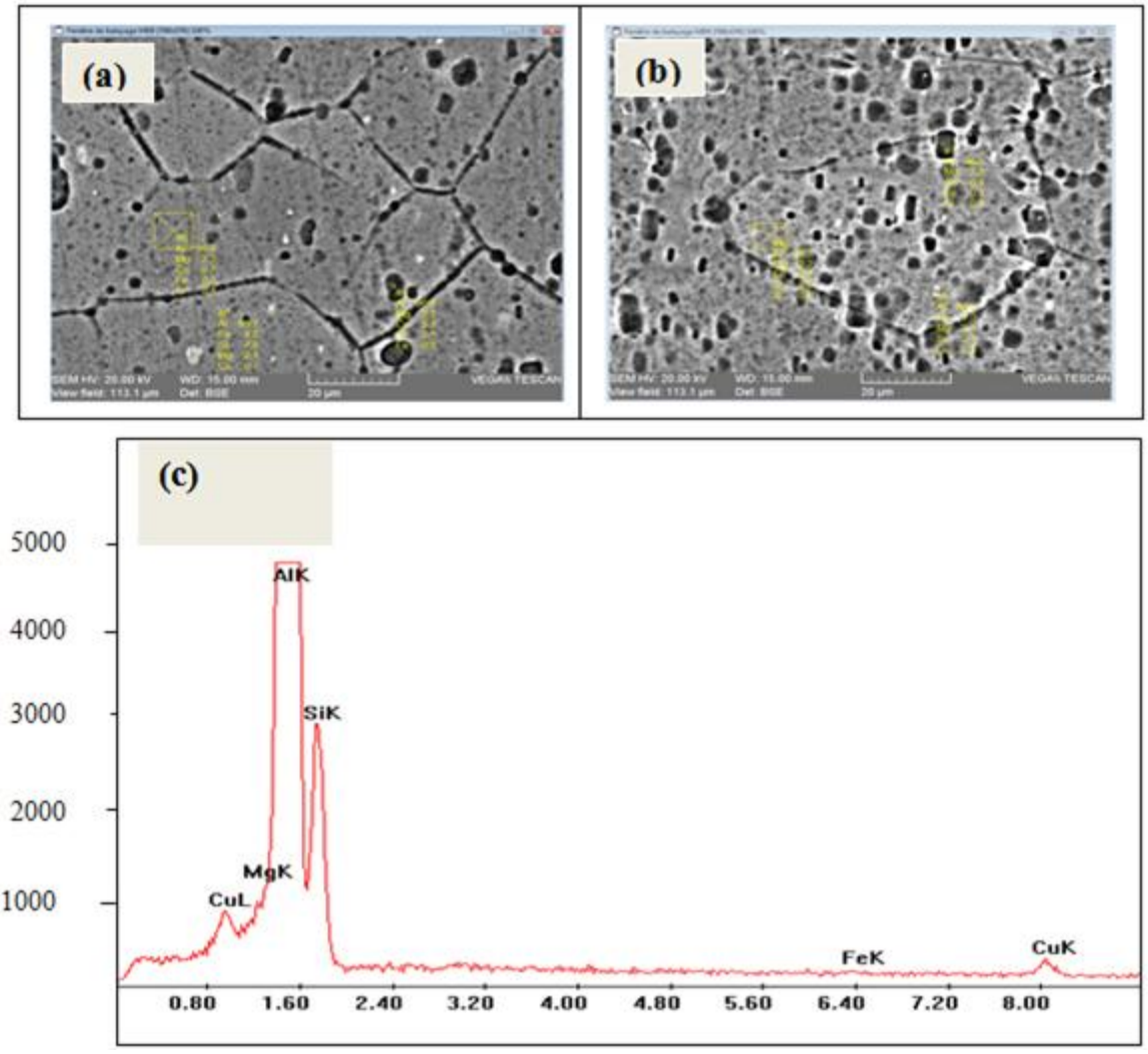

Figure 5. (a) SEM micrograph of the 30% cold rolled sample, (b) SEM micrograph for the same sample after aging at 175 °C for 30 min, (c) EDS spectrum of particles shown in the image 5b.

Figure 5b shows an increase of the precipitates density in α-aluminium matrix grains, after aging at 175 °C for 30 min. These fine particles are also attributed to the Mg_2Si phase. Figure 5c illustrates the EDS spectrum of particles seen in Figure 5b. They contain a high amounts of Si and Mg with Al. This is an indicator of the formation of β" or β'-type precipitates which is in good agreement with DSC results (Figure 3) and others reported elswhere [20-24].

3.3. Influence of aging on mechanical properties

3.3.1. Hardness

The DSC experiment indicates that the β" precipitation reaction occurs at a temperature of about ˜240 ° C for the homogenized alloy and quenched without cold deformation. This leads to studying the isothermal aging behavior (240 °C) for this alloy. Figure 6 shows the variation of the hardness values as a function of the artificial aging time at different aging temperatures of the studied alloy. We have considered in this study the homogenized and quenched sample which was artificially aged at 175 and 240°C and two deformed states; i.e. 20% and 30% cold rolled samples, submitted to aging at 100°C.

. The hardness curves indicate that although the maximum hardness value (82 Hv) was recorded after artificial aging at 240 °C for 30 min, a prolonged aging for 10h at 175 °C gave a hardness value greater than 95 Hv in the chosen period of time.

Isothermal aging at 100 °C for 30 min revealed that the hardness values have maximums of 87 and 97 Hv for the 20% and 30% cold rolled samples, respectively. Isothermal aging (100 °C) beyond one (1h) leads to a slight decrease in hardness for the two cold rolled samples that can be attributed to the dissolution of GP zones formed during natural aging. It should be noted that aging time of 10h at 100 °C is not sufficient to cause a major recovery of the deformed structure that can cause a drop in hardness.

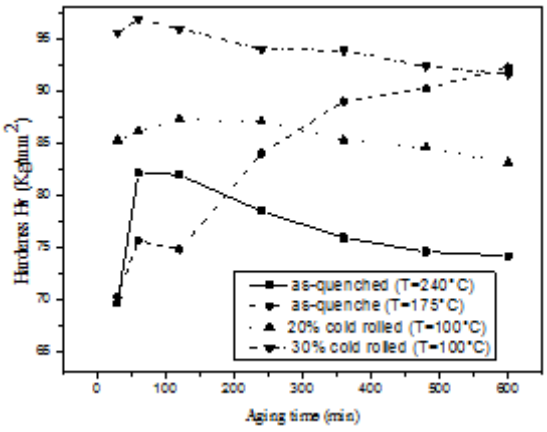

Figure 6. Variation of the hardness values with the aging time at different artificial aging temperatures of the studied alloy treated under different conditions.

Figure 7 shows the change in microhardness values as a function of natural aging time of the studied alloy for three states: homogenized and quenched, the 20 and 30% cold rolled samples. The results show that the maximum hardness value, 77 Hv, can be obtained after 10 days for the homogenized and quenched sample, against 83 Hv for the 20% cold rolled sample after 3 days only of aging. Increasing the cold deformation rate from 20% to 30% increases the maximum hardness value to 95 Hv. The hardness of the as quenched sample increases and reaches a plateau after 6-9 days while it decreases for the 30% cold rolled sample which reaches the plateau after 12 days. However, it remains stable for the 20% cold rolled state. The presence of a plateau is because there is not enough free solute and gaps in the deformed alloys to allow a new precipitation so the process stops almost after few days.

Effectively, Martinsen et al., reported that after heat treatment, the aluminum materials are usually stored for more than one week at room temperature before being put into further application, during which aluminum undergoes a natural aging process [27].

It is mentioned that the maximum hardness value of 97 Hv for the 30% cold rolled state is reached mainly because of the work hardening effect and not linked to the precipitation during natural aging. Therefore, it could be mentioned that cold deformation before aging is ineffective for the kinetic of natural aging.

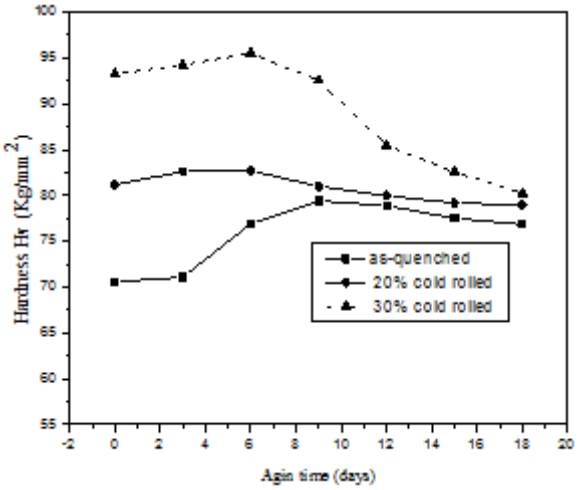

Figure 7. Variation of the hardness values with the natural aging time of the: homogenized and quenched alloy, 20 and 30% cold rolled samples.

It is evident from figures 6 and 7 that the hardness values have steadily increased with increasing cold deformation. Our observations are in agreement with results of Jin et al. which suggest that natural aging has a much lower influence on hardness of pre-deformed samples [14].

3.3.2 Tensile properties

Table 3 summarizes tensile properties of the studied alloy. It gives values of yield strength (YS), tensile strength (UTS) and total elongation (TEL) of a casting

(at 500°C) and water quenched sample (before and after natural aging of 7 days), 20% and 30% cold rolled specimens which are also subjected to natural aging for 7 days.

The as casted alloy presents the lowest YS (85 MPa) and UTS (91 MPa) with the greater total elongation (about 2%). After natural aging, The YS and UTS values increses to 130 and 170 MPa, respectively, while the taotal elongation decreases to 1.77. This evident hardening is probably due to Mg and Si atoms that start to precipitate after quenching or to form clusters immediately during Natuaral aging [28, 29].

Aging of 20% and 30% cold rolled samples leads to higher values of YS (182 and 209 MPa, respectively) and UTS (213 and 237 MPa, respectively) with a lose of ductility (TEL is 1.18% for 30% deformed sample) after a natural aging. This strengthening occurs because of dislocation movements and dislocation generation within the crystal structure by interaction between the existing particles [23].

The increase of YS and UTS with simultaneous decrease of the elongation in the deformed alloys is mainly due to the increase of strain and not to precipitation hardening effect. The difference between UTS and YS for the 20% and 30% deformed alloys which are subjected to natural aging is probably weak compared to the naturally aged alloy. This result suggests that the natural aging of the cast sample becomes more efficient also with respect to the cold-deformed sample to improve tensile properties.

Table 3 : Tensile test results of the investigated samples

Type of treatment	YS/MPa	UTS/Mp	TEL/ %
quenched cast sample	85	92	2.05
quenched, natural aging 7d	130	170	1.77
20%, natural aging for 7 d	182	209	1.43
30%, natural aging for 7 d	210	227	1.18

4. Conclusion

In this paper, metallographic SEM and optical microscopy, DCS curves, hardness and tensile measurements have been applied to investigate the precipitation processus and the effect of cold deformation on the mechanical properties upon natural and artificial aging of an Al-Mg-Si alloy. The Kissinger method has been used to estimate the activation energy of β-phase precipitation. The most relevant conclusions are :

- DSC study indicates that precipitation of β-phase, after homogenization, occurs in the temperature range 240-255°C. The estimated activation energy value for the above reaction, using Kissinger method, is about 83.1 kJ /mol.
- Fine precipitates of β-phase embedded in the α-aluminium matrix were observed of the deformed and aged samples.
- The as quenched state samples showed that the precipitation hardening is obvious.
- The 20% and 30% cold deformations before aging contributed to the aging response. The increase in hardness and tensile strength with the simultaneous decrease of elongation in the deformed alloy is mainly due to the strain strengthening and no to precipitation hardening.

References

[1] A. K. Gupta, D. J. Lloyd, S. A. Court, Mate. Sci. Engi. A301 (2001) 140-146
[2] A. K. Gupt a, D. J. Lloyd, S. A. Court, Mater. Sci. Engi. A316 (2001) 11-17
[3] W. Chrominski, M. Lewandowska, Acta. Mate. 103 (2016) 547-557
[4] D. J. Chakrabarti, D. E. Laughlin, Prog. Mater. Sci. 49 (2004) 389-410
[5] L. Blaz, E. Evangelista, Mater. Sci. Engi. A207(1996) 195-201
[6] Y. Birol, M. Karlik, Scripta. Mater. 55 (2006) 625-628
[7] M. Vaseghi, H. S. Kim, Mater. Design. 36 (2012) 735-740
[8] E. Cerri, P. Leo, Mater.Sci. Engi. A 410 (2005) 226–229
[9] D. Jiang, C. Wang, Mater. Sci. Engi. A352 (2003) 29-33
[10] H. J. Roven, M. Liu, J. C. Werenskiold, Materi. Sci. Engi. A 483 (2008) 54-58
[11] S. K. Ghosh, J. Mater. Sci. Techno. 27 (2011) 193-198
[12] Y. N. Kwon, Y. S. Lee, J. H. Lee, J. Mater. Proc. Tech 187 (2007) 533-536
[13] C. D. Marioara, S. J Andesen, H. Jansen, H.W. Zandbergen: *Acta Mater.*, 2003, 51, 789–796.
[14] S. Jin, T. Nagi, L. Li, S. Jia, T. Zhri, D. Ke: *Materials.*, 2018, 11,1422-1434.
[15] H. E. Kissinger: *Anal. Chem.*, 1957, 29, 1702.
[16] G. A. Edwards, K. Stiller, G. L. Dunlop, M. J. Couper, Acta. Mater. 46 (1998) 3893-3904
[17] S. Nayebossadri, J. Speight. D. Book, J. Membra. Sci. 451 (2014) 216-225
[18] S. Abis, M. Massazza, P. Mengucci, G. Riontino, Scripta. Mater. 45 (2001) 685-691.
[19] B. K. Prasad, A. K. Jha, O. P. Modi, S. Das, R. Dasgupta, J. Mater. Sci. Lett. 17 (1998) 1121-1128
[20] H. Wu, S. P. Wen , H. Huang, X. L.Wu, K. Y. Gao, W.Wang, Z. R. Nie, Mater. Sci. Eng. A 65 (2016) 1415-424
[21] H. Liao, Y. Wu, K. Zhou, J. Yang, Mater. Des. 65 (2015) 1091-1099
[22] X. Kai, C. Chen, X. Sun, C. Wang, Yu. Zhao, Mater. Des. 90 (2016) 1151-1158
[23] T. Saito, C. D. Marioara, J. Royset, K. Marthinsen, R. Holmestad, Mater. Sci. Eng. A609 (2014) 72-79
[24] X.Wang, M. Guo, Y. Zhang, H. Xing, Y. Li, J. Luo, J. Zhang, J. A. Comp. 657 (2016) 906-916

[25] H . Ezuber, A . H oud, F. Shawesh, Materi. Des. 29 (2008) 801-805

[26] Yan Zheng, Wenlong Xiao, SujingGe , Weitao Zhao , Shuji Hanada , Chaoli Ma : *J. A. Comp*, , 649, (2015)291–296.

[27] F. A. Martinsen, F. J. H. Ehlers, M. Torsæter, R. Holmestad: *Acta Mater.* , 60, (2012)6091–6101

[28] C. D. Marioara, H. Nordmark, S. J. Andersen, R. Holmestad: *J. Mater. Sci.*, , 41, (2006)471–478

[29] Y. Aruga, M. Kozuka, Y. Takaki, T. Sato: *Mater. Sci. Eng. A.*, , 631, (2015)86–96.